Important Factors for Computational Modeling of UV Disinfection Systems

Clifford K. Ho and Siri S. Khalsa
Sandia National Laboratories, Albuquerque, NM, ckho@sandia.gov

Ed Wicklein
Carollo Engineers, Seattle, WA

Harold Wright
Carollo Engineers, Boise, ID

ABSTRACT

This paper presents computational fluid dynamics models of UV disinfection systems for water treatment. Hydraulic, radiation, and dose-response models are used to elucidate important features, processes, and parameters that impact the simulated performance of UV reactors. Sensitivity analyses are presented that investigate the impact of different particle tracking models and parameters. Results show that discrete random walk models can be impacted by system conditions such as flow rate and model parameters such as the number of particles injected. The impact of wall reflection on radiative transfer within the reactor is also investigated, and results show that wall reflection can significantly increase the simulated dose in water with high UV transmittance. Evaluation of different pipe configurations and their impact on the simulated approach hydraulics and system performance is also investigated.

INTRODUCTION

The performance of ultraviolet (UV) disinfection systems can be impacted by a number of factors that affect the hydraulics and/or UV intensity fields in these systems. Some of these factors (e.g., flow rate, UV transmittance) are characterized during validation testing of the UV reactors. However, the impacts of these and other factors, such as variability in UV lamp configuration and changes to the inlet/outlet piping, can be difficult to characterize if the installed configuration is different than the validated configuration. In many cases, utilities will be retrofitting UV into existing treatment systems, so they may be limited in their ability to either match the validated configuration or fully characterize the installed configuration. Thus, utilities need a tool to assess the impact of factors that may affect the hydraulics or UV intensity fields in their systems. Moreover, a better understanding of the effects of inlet/outlet hydraulic configurations and lamp configurations on UV disinfection performance will result in more pragmatic design recommendations, with a potential to significantly reduce capital costs in future UV installations.

This study presents the results of sensitivity analyses using computational fluid dynamics (CFD) models and CFD-based UV dose models. As prescribed in the United States Environmental Protection Agency's UV Disinfection Guidance Manual (UVDGM), CFD modeling and CFD-based dose modeling may be used to assess the performance (dose delivery) of installed systems relative to validated systems. In addition, the UVDGM states that these models may be used to

develop theoretical dose monitoring equations, which may be useful when the range of operating or design conditions falls outside the validated conditions. Sensitivity analyses were conducted to determine important factors that impacted the simulated reduction equivalent dose (RED), which was used as the performance metric in computational models of validated commercial reactors. Features modeled in the simulations included different pipe configurations, lamp configurations, flow rates, and UV transmittances. In addition, factors relevant to computational modeling of UV disinfection systems were also considered, such as the impact of grid resolution, particle tracking methods, and features of the UV intensity model. The identification of these important features and processes will enable engineers and regulators to improve the development, evaluation, and interpretation of CFD-based models for UV disinfection systems.

DESCRIPTION OF COMPUTATIONAL MODELS

Two commercial UV reactors were simulated in this study: the Infilco Degremont Inc. (IDI) Aquaray® H_2O 20" UV Disinfection Reactor and the Calgon Carbon Corporation (Calgon) 12" Sentinel UV Reactor. Validation reports for each of these reactors were provided by the manufacturers.

IDI Aquaray H_2O 20" Reactor. The IDI Aquaray (Ozonia) reactor was modeled using two configurations, the M-rig, which utilized a single reactor installed in 12-inch piping, and the L-rig, which utilized two reactors in series installed in 24-inch piping.

The M-rig model, shown in Figure 1, started with a section of straight 12-inch diameter pipe 60-inches long (5 pipe diameters), leading to a 90-degree elbow. The piping then ran straight to a S-bend, which included two 90-degree elbows separated by a short spool section. The S-bend was followed by a concentric expansion, which connected to the reactor. The reactor included 6 lamp sleeves, the wiper power screw, the outside surfaces of the sensors, and baffles. A concentric reducer is located downstream from the reactor, followed by approximately 5 diameters of 12-inch diameter straight piping. For some test conditions a porous baffle plate was located within the piping between the concentric expansion and the reactor.

The L-rig model, shown in Figure 2, began with a section of straight 24-inch diameter pipe 120-inches (5 pipe diameters), leading to a S-bend, which included two 90-degree elbows, separated by a short spool section. The S-bend was followed by a concentric reducer, which was attached to the upstream reactor. A second reactor was attached to the downstream end of the first reactor and followed by a concentric expansion back to 24-inch diameter pipe, which ran straight for approximately 5 diameters to the model outlet.

For both the M-rig and L-rig model runs, a similar procedure was used to generate the model grids. The piping was meshed using GAMBIT primarily with hexahedral elements using a Cooper scheme, which includes boundary layer elements at the surface. The M-rig had 1,120 cells along the pipe cross section, and the L-rig utilized 1,092 cells along the pipe cross section. The pipe elements were held constant with a minimum cell dimension of 10 mm for the M-rig, and 20 mm for the L-Rig for each case.

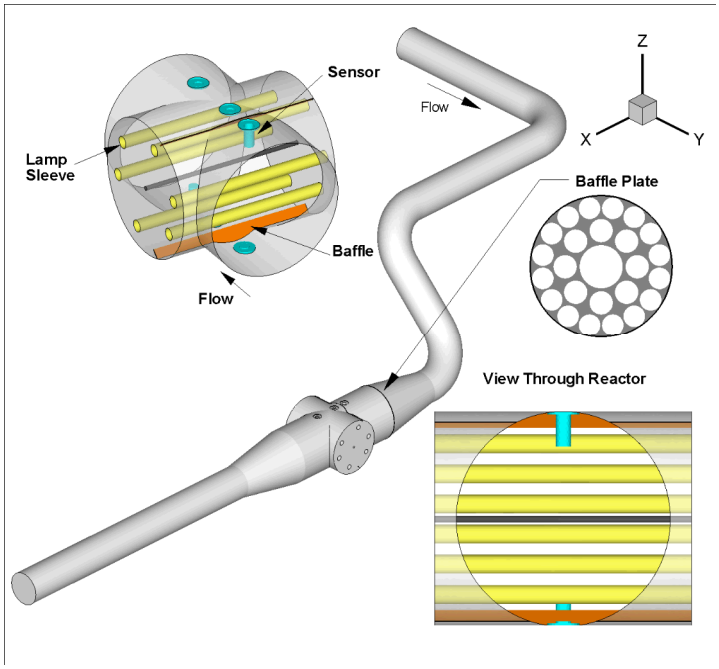

Figure 1. M-rig GAMBIT/FLUENT model of the IDI Aquaray (Ozonia) reactor and piping.

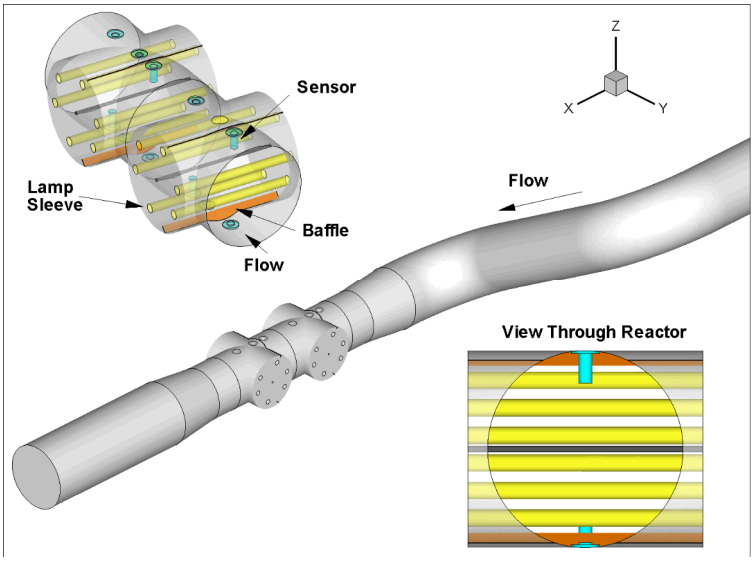

Figure 2. L-rig GAMBIT/FLUENT model of the IDI Aquaray (Ozonia) reactor and piping.

A grid sensitivity analysis was performed by progressively refining the reactor model grid until hydraulic and performance metrics no longer changed. Details of the grid sensitivity study can be found in Wicklein et al. (2008, this proceedings).

Calgon 12" Sentinel Reactor. The Calgon Sentinel reactor was modeled in a 12-inch diameter pipe. The complete model domain is shown in Figure 3. The model began with a straight pipe section approximately 10 pipe diameters long. The straight piping was followed by a single 90-

degree elbow approximately 4 pipe diameters upstream from the reactor. The reactor included the outer surface of the lamp sleeves, the sensor bodies, and included both horizontal and vertical baffles to director flow toward the lamps. A second 90-degree elbow was located approximately 1 diameter downstream from the reactor, followed by a concentric expansion to 18-in diameter pipe.

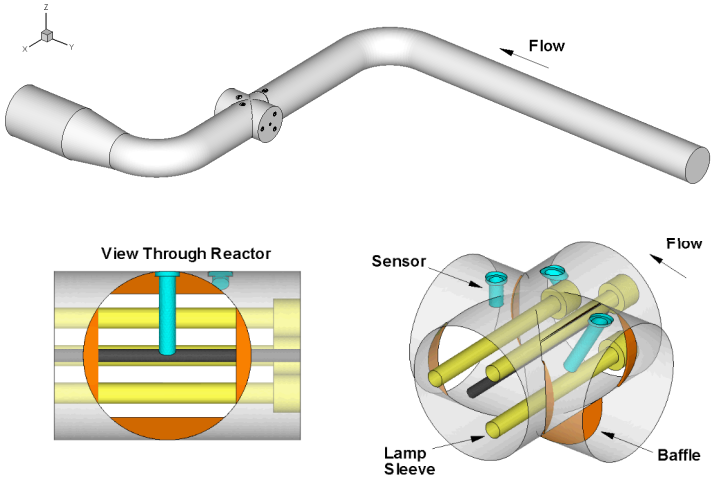

Figure 3. GAMBIT/FLUENT model of the Calgon Sentinel reactor and piping.

The pipes were meshed with hexahedral elements using a Cooper scheme and included boundary layer elements at the surface. A grid sensitivity analysis was performed by progressively refining the model grid within the reactor. For all cases the pipes included 249,500 elements, ranging in size from 0.25-inches to 2 inches. The reactor was meshed using a tetrahedral/hybrid mesh with a hexahedral core. Details of the grid sensitivity study can be found in Wicklein et al. (2008, this proceedings).

Hydraulic Model. The computational fluid dynamics (CFD) software FLUENT was used to simulate the hydraulic conditions within the UV disinfection systems. An inflow velocity was applied at the upstream end of the model using a uniform velocity distribution corresponding to the respective test conditions. The downstream boundary was an outflow boundary. All other surfaces were wall boundaries. The κ-ε realizable turbulence model was used in all cases, with the standard wall function. The models were all run to steady state in double precision. The solution was calculated with the SIMPLE algorithm utilizing a second order accurate dicratization. The models were run to a converged solution, defined by an absolute residual of less than 0.001 for all solved variables.

After the flow solution converged for each of the reactor models, particles were released at the inlet and tracked in time as they traveled through the system. Particle tracking was performed both with and without the discrete random walk model as part of the sensitivity analyses. The particle paths were used in conjunction with the UV radiation model described in the next section to determine a dose distribution.

UV Radiation & Dose Models. The discrete ordinates (DO) radiation model in FLUENT solves the radiative transfer equation over a domain of discrete solid angles. It calculates the radiation intensity as a result of absorption, scattering, and emission within the fluid, along with reflection and emission from surfaces within the fluid. Because it is implemented within the FLUENT CFD code, the impacts of geometry within the reactor (e.g., shadowing, reflection) can also be readily considered. In addition, a user-defined function (UDF) was implemented to calculate the cumulative dose of particles moving through the reactor. The cumulative dose (J/m^2) was calculated as the product of the irradiation (W/m^2) and the exposure time (s) at each step along the particle path.

A previous study by Liu et al. (2004) concluded that the discrete ordinates model over predicted the intensity close to the lamps but under predicted the intensity far from the lamps because it did not include refraction. Refraction at interfaces *can* be included in the FLUENT discrete ordinates model, but the interfaces and geometries of different materials (e.g., lamp, air annulus, quartz sleeve) need to be discretely modeled.

Dose Response Curves. The dose associated with each particle path was converted to an equivalent inactivation and reduction equivalent dose (RED) using appropriate dose-response curves. For the IDI Aquaray tests, B. subtillis was used, and for the Calgon Sentinel tests, MS2 Phage was used. Dose-response curves took the following forms for these tests:

IDI Aquaray: $\log(N/No) = A - B \times (\text{Dose in } J/m^2)$

Calgon Sentinel: $\text{Dose } (mJ/cm^2) = A \times \log(No/N) + B \times \log(No/N)^2$

where A and B are fitting coefficients provided in the validation reports, No is the number of viable microbes introduced to the system, and N is the number of viable microbes remaining after exposure to the UV reactor. Thus, N/No is the survival ratio, and No/N is the inactivation ratio. The procedure for determining RED from a distribution of particle doses can be found in Munoz et al. (2007).

SENSITIVITY ANALYSES

Sensitivity analyses were performed using the modeled UV reactors to investigate the impact of various particle tracking inputs and wall reflection. The impact of different pipe configurations on hydraulics and simulated RED was also investigated.

Particle Injection and DRW. A sensitivity analysis was performed to expand on the work performed by Munoz et al. (2007) to investigate the impacts of various particle tracking inputs on the simulated performance (RED) of addition UV reactors. The number of injected particles required to ensure a sufficiently invariant simulated RED is investigated. Furthermore, when the Discrete Random Walk (DRW) model is enabled for the particle tracking calculations, variability is observed among repeated runs. With DRW enabled, a random fluctuating velocity component (caused by turbulence) is added to the mean velocity at each time step along the particle trajectory. Therefore, for different runs (tries), a particle will take different paths with DRW enabled. This study also seeks to determine the number of repeated runs (tries) required to obtain a sufficiently invariant mean simulated RED.

Two geometries were considered in this study using the IDI Aquaray UV reactor: (1) L-rig without baffle, only reactor #1 turned on and (2) M-rig without baffle. Two test conditions with different flow rates were chosen for each geometry and simulated in FLUENT. The particle tracking model was run on each of the 4 configurations using 10 different injection files (ranging from ~200-50,000 injection points). For each configuration, each injection file was run once without DRW and 20 times with DRW enabled. For both geometries, a high flow rate and a low flow rate test were chosen, as the DRW Sensitivity Study concluded that the effect of the velocity fluctuations introduced by the DRW model varies inversely as the flow rate.

The lamp irradiation boundary condition for each case was fixed at a value that would, with DRW enabled, yield a simulated RED close to the measured RED. No wall reflection was simulated. The Random Eddy Lifetime option of the DRW model was enabled in this study, which randomized the characteristic eddy lifetime. For one configuration, a comparison was made between the simulated REDs yielded from enabling and disabling Random Eddy Lifetime. Table 1 summarizes the test conditions chosen for this sensitivity analysis:

Table 1. Summary of test conditions for particle injection sensitivity study.

Test ID	Geometry	Flow Rate (m^3/h)	Test UVT	Nominal Test Lamp Power (kW)	Measured RED (J/m^2)
AM	L-rig, reactor #1	380	81.85%	24	511
BD	L-rig, reactor #1	2050	91.83%	24	304
AF	M-rig no baffle	420	81.85%	24	390
P	M-rig no baffle	1200	90.36%	24	325

Figure 4 through Figure 7 show the simulated RED for each of the four reactor configurations using different configurations of particle tracking inputs. The simulated mean RED is plotted against the number of particles that were injected and traveled through the system for each run. For multiple runs (tries), the same number of particles was injected for each run (try). In each plot, simulations with and without DRW enabled are shown.

Results show that there is a notable difference between the simulated RED with and without DRW, and this difference appears to be more pronounced at lower flow rates. This difference will be further explored in the sensitivity analysis that follows. It should be repeated that the simulated lamp output was calibrated using the runs with DRW enabled, so it is expected that the simulated RED with DRW enabled will match the observed RED values listed in Table 1. The variability of the simulated RED also appears more dependent on the number of injected particles when the flow rate is low, where a greater number of particles yields lower variability in the simulated RED between tries. Also, with increased numbers of tries, the variability is reduced, even with fewer particles injected.

In all cases, the variability in the simulated RED drops to less than several percent if greater than 5,000 - 10,000 particles is used for any number of tries. Even in the case of the lowest flow rate, Test AM (flow rate 380 m^3/h), the % Error in Mean RED was within 1% for any number of tries when near 14,000 particles were used.

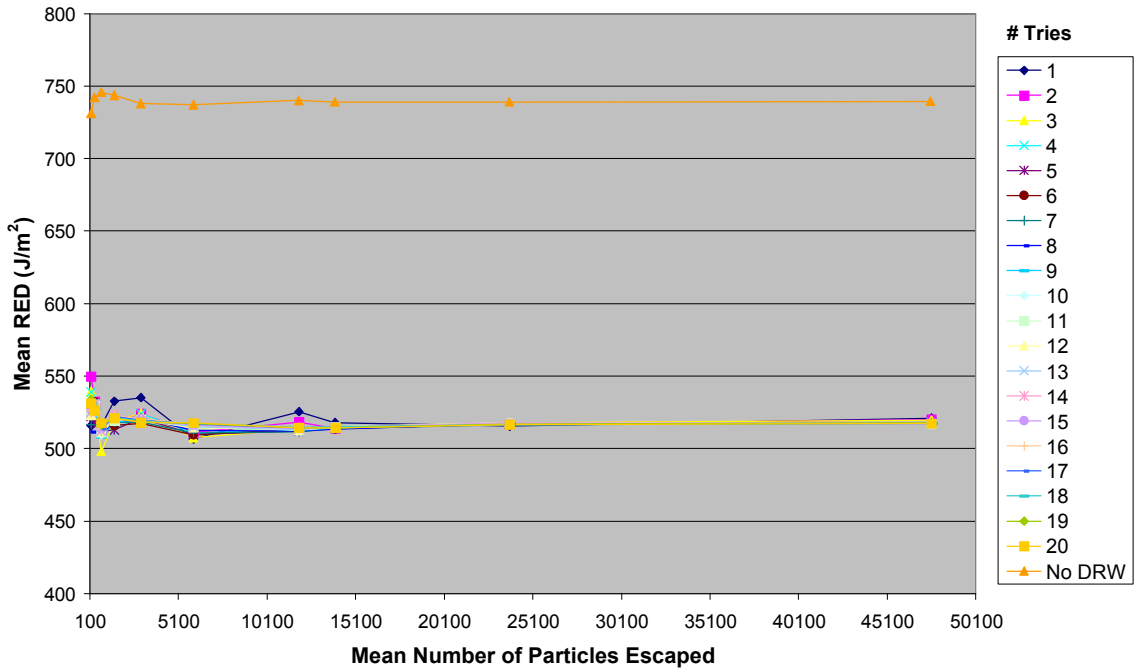

Figure 4. Simulated mean RED for different particle injection configurations for the L-rig, Test AM, 380 m^3/h, UVT = 81.85%.

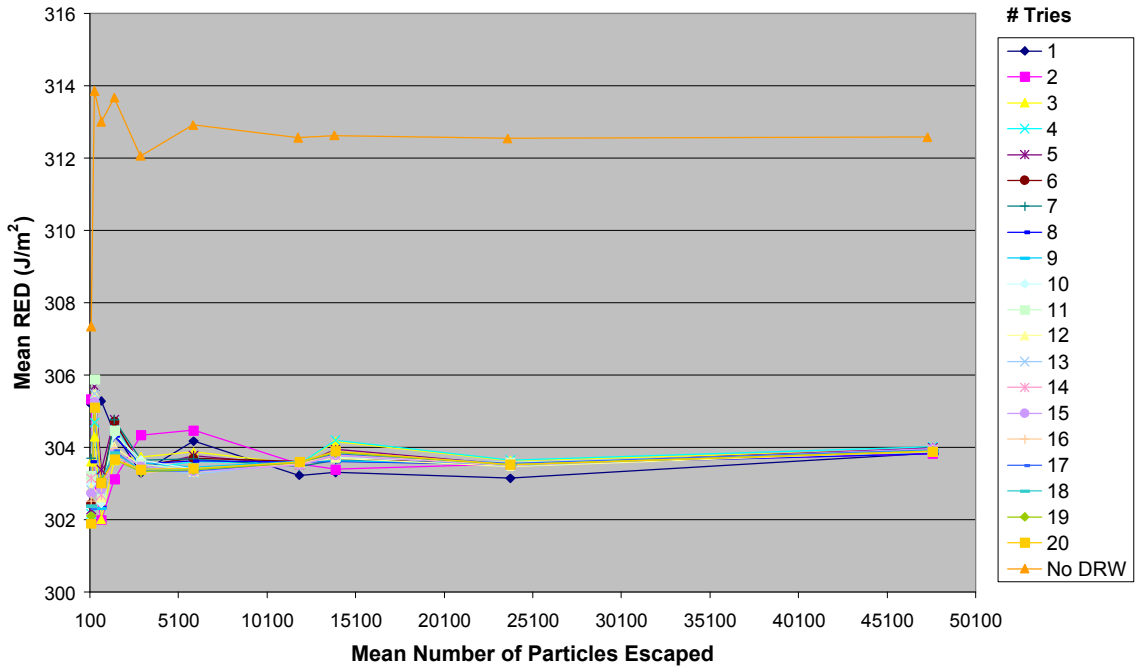

Figure 5. Simulated mean RED for different particle injection configurations for the L-rig, Test BD, 2,050 m^3/h, UVT = 91.83%.

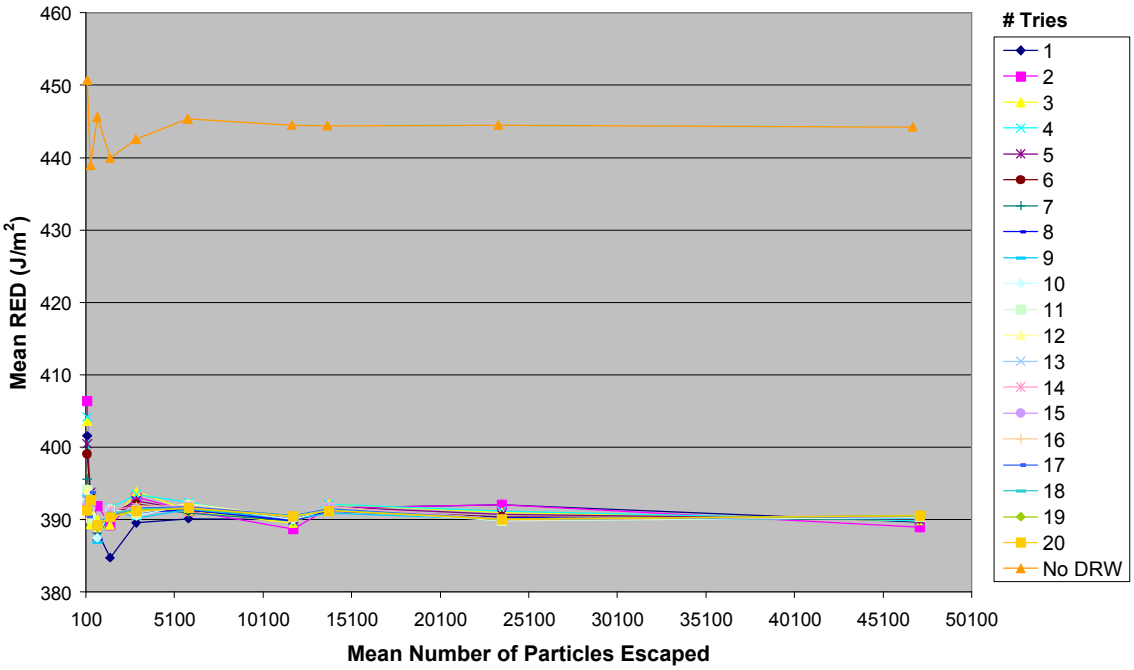

Figure 6. Simulated mean RED for different particle injection configurations for the M-rig, Test AF, no baffle, 420 m^3/h, UVT = 81.85%.

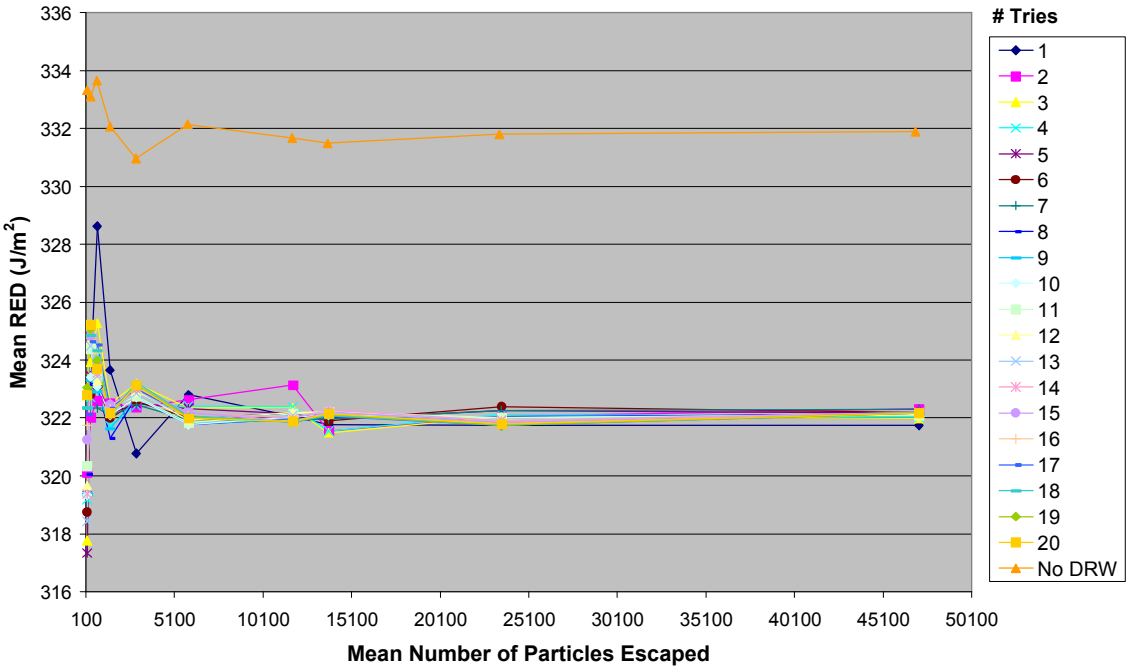

Figure 7. Simulated mean RED for different particle injection configurations for the L-rig, Test P, no baffle, 1,200 m^3/h, UVT = 90.36%.

The test condition M-rig No Baffle Test AF (Flow Rate 420 m^3/h, UVT = 81.85%) was run using nearly 14,000 particles, 20 tries with DRW, and with Random Eddy Lifetime, and 20 tries with DRW but without Random Eddy Lifetime (hence with Constant Eddy Lifetime). Test AF had a sufficiently low flow rate for the DRW model to have a notable impact on the simulated RED, yet the difference between REDs for Random and Constant Eddy Lifetime was within 0.7% for any number of tries. The choice of enabling vs. disabling Random Eddy Lifetime thus appears inconsequential.

Impact of DRW vs. flow rate. The previous sensitivity study indicated that the difference between simulated RED values with and without DRW enabled was more pronounced at lower flow rates. This sensitivity study is intended to confirm this behavior and elucidate the reasons by investigating a greater number of test runs with different flow rates and configurations. Three different geometries were considered in this study: (1) L-rig without baffle, only reactor #1 turned on, (2) M-rig without baffle, and (3) M-rig with baffle.

Four test conditions with different flow rates were chosen from each series and simulated in FLUENT. The lamp irradiation boundary condition was not calibrated to any of the measured REDs and was fixed at 4 kW/m^2 for each of the six sleeves. No wall reflection was simulated. 14,010 particles for L-rig and 13,833 particles for M-rig injected uniformly across the inlet were tracked. The particle tracking model was run once without DRW and 3 times with DRW. The Random Eddy Lifetime option of the DRW model was enabled in this study, which randomized the characteristic eddy lifetime. The table below details the test conditions chosen for this study:

Table 2. Summary of test conditions for DRW vs. flow rate sensitivity study.

Test ID	Geometry	Flow Rate (m^3/h)	Test UVT	Nominal Test Lamp Power (kW)	Measured RED (J/m^2)
AM	L-rig, reactor #1	380	81.85%	24	511
AP	L-rig, reactor #1	890	86.70%	24	380
BC	L-rig, reactor #1	1200	87.10%	24	310
BD	L-rig, reactor #1	2050	91.83%	24	304
AF	M-rig no baffle	420	81.85%	24	390
AI	M-rig no baffle	890	86.70%	24	320
M	M-rig no baffle	600	85.31%	24	372
P	M-rig no baffle	1200	90.36%	24	325
AD	M-rig with baffle	440	82.99%	24	464
AE	M-rig with baffle	660	86.70%	24	432
AL	M-rig with baffle	950	91.83%	24	511
BG	M-rig with baffle	800	87.10%	24	353

Results showed that for all three reactor configurations, the simulated difference between the RED values resulting from runs with and without DRW enabled was inversely proportional to the flow rate (Figure 8). At lower flow rates, the difference was between 15 - 35% for the

three different reactor configurations. At higher flow rates, the simulated difference decreased to below 5%.

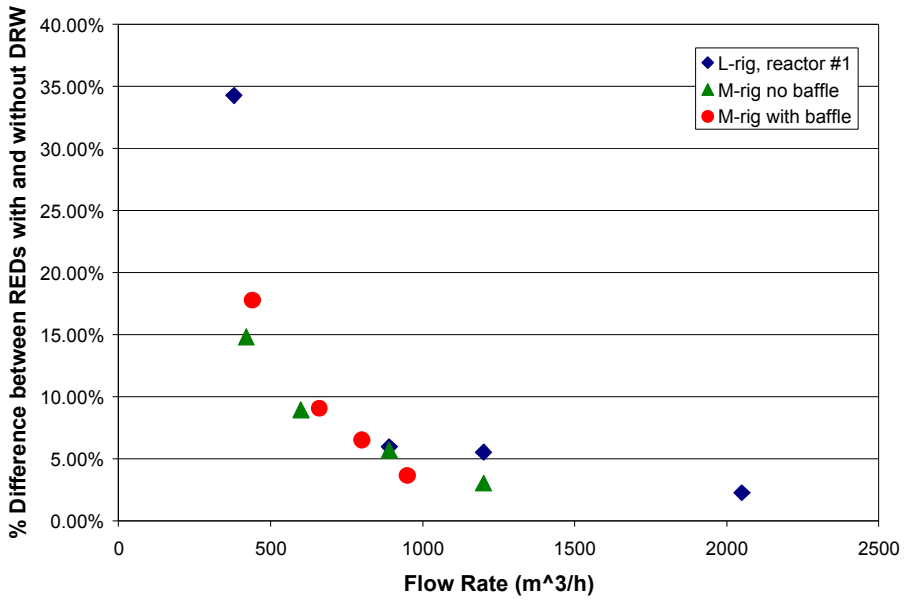

Figure 8. Percent difference between simulated RED values from runs with and without DRW enabled as a function of flow rate for different reactor configurations.

The REDs with and without DRW converged as the flow rate increased, for all three geometries. A possible explanation for this behavior is that the turbulent random velocity fluctuations that are added to the mean velocity components in the DRW model are more significant relative to the mean velocity components at lower flow rates. The components of the turbulent velocity fluctuations introduced by the DRW model are given by:

$$u' = \zeta\sqrt{2k/3}$$
$$v' = \eta\sqrt{2k/3}$$
$$w' = \xi\sqrt{2k/3}$$

where ζ, η, and ξ are Gaussian random numbers, and k is the turbulent kinetic energy. Hence, we would expect this explanation to be true if the ratio of the square root of the turbulent kinetic energy to the mean velocity magnitude was found to be inversely proportional to the flow rate. Figure 9 shows this ratio (the volume-averaged square root of the turbulent kinetic energy to the volume-averaged velocity magnitude for a fluid region enclosing the reactor) as a function of flow rate. The results confirm that the turbulent kinetic energy and, hence, the turbulent velocity fluctuations, are more significant at lower flow rates. Differences between runs with and without DRW enables are therefore expected to be larger at lower flow rates.

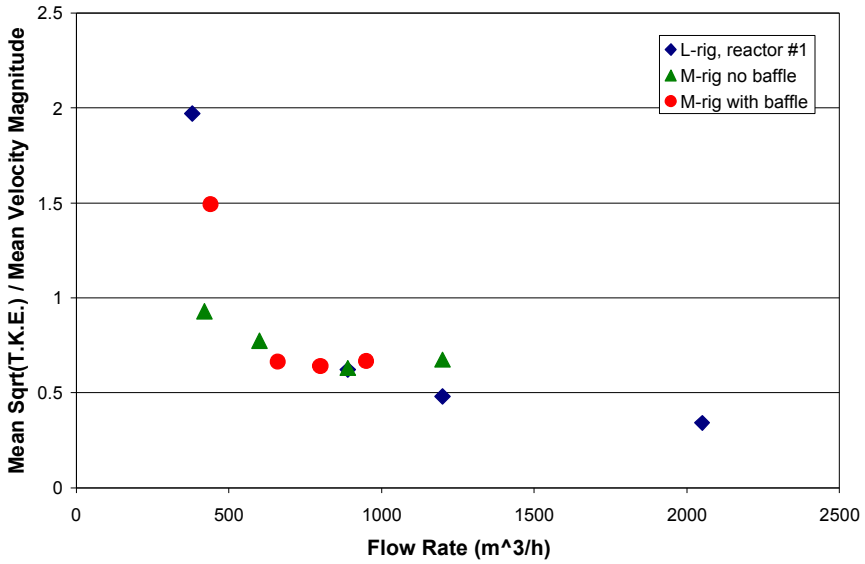

Figure 9. Simulated ratio of the mean turbulent kinetic energy to the mean velocity magnitude as a function of flow rate for different reactor configurations.

Wall reflection. Many radiation models (e.g., lines source integration, multiple points source summation, multiple segment source summation) that are implemented separately from the CFD model often neglect the influence of wall reflection in their calculations. Because the DO radiation model in FLUENT can readily account for reflection from features within the reactor (e.g., sensors, sleeves, walls), it was used in this analysis to determine the potential importance of reflection on the UV intensity distribution.

Two configurations of the Calgon 12" Sentinel were evaluated to perform sensitivity analyses using the Fluent DO radiation model: (1) UVT = 88% (ID #57) and (2) UVT = 98.6% (ID #46). A simulated lamp output of 2,700 W/m^2 applied to each sleeve was found to yield a good match with the observed RED for a UVT of 88%. This lamp output was then used for all subsequent runs and configurations.

Figure 10 shows a plot of simulated radiation intensities using Fluent with and without wall reflection for UVT = 88% and UVT = 98.6%. For the simulation with wall reflection, the internal emissivity for the reactor walls was changed from 1 to 0.6, which yields a 40% reflectivity. A value of 40% was used based on the spectral reflectance at 254 nm reported in Luckiesh (1929) for polished steel (however, recent personal communication with Keith Bircher at Calgon Carbon Corporation indicated that this value should probably be lowered to ~20%). Reflection from the walls was assumed to be completely diffuse (diffuse fraction = 1) because they were bead blasted.

At UVT = 88%, the impact of wall reflections was found to be small (but still noticeable) relative to the differences when UVT = 98.6%. At UVT = 98.6%, the simulation with wall reflection yields UV intensities that are up to 100% greater than the simulation without wall reflection at

locations near the walls and near the center of the reactor between the lamps (Figure 10). Figure 10 also shows a notable impact of shadowing from the wiper screw in the center of the reactor.

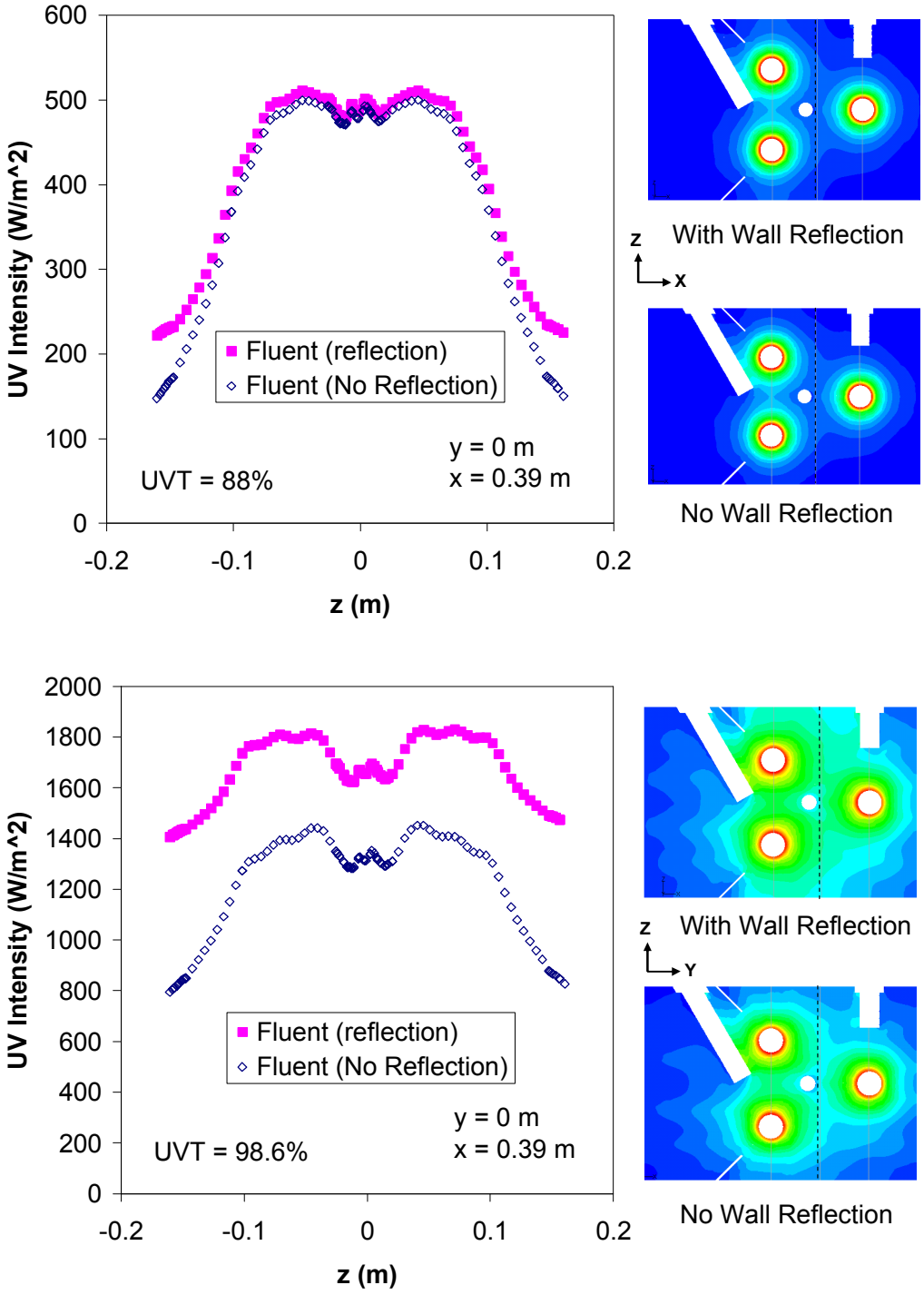

Figure 10. Comparison between simulated UV intensities along a vertical transect (x=0.39m) in the Calgon reactor using Fluent with and without wall reflection. Top: UVT = 88%, Bottom: UVT = 98.6%.

Error! Reference source not found. shows the simulated cumulative dose along particle paths with and without reflection for a UVT = 98.6%. The wall reflection increases the amount of irradiation received by the particles, so the simulated cumulative dose distribution is higher. Note that in these simulations, DRW was not enabled to ensure repeatability between runs with and without wall reflection. Particle paths with DRW would be more random and less uniform.

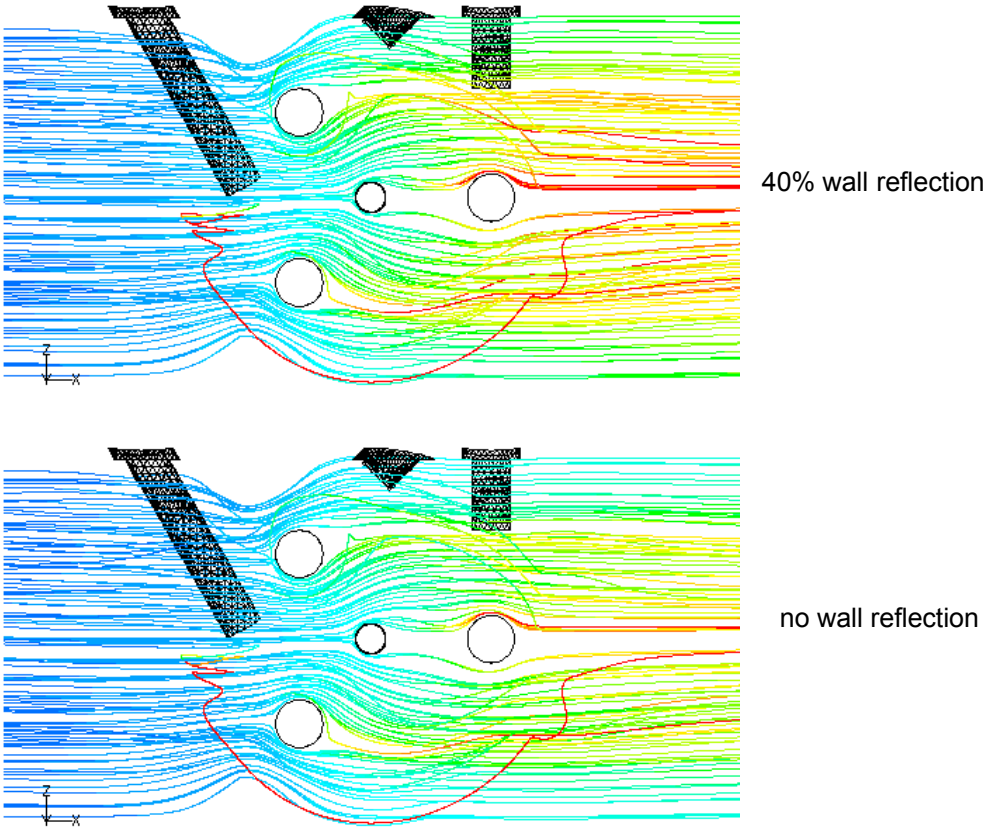

Figure 11. Simulated cumulative dose (red is high, blue is low) of individual particles released into the Calgon Sentinel reactor using the discrete ordinates radiation model with UVT = 98.6%. Top: 40% wall reflection, Bottom: no wall reflection.

Figure 12 shows the measured and simulated RED using Fluent with and without reflection for UVT = 88% and UVT = 98.6%. Because the lamp power (2,700 W/m^2) was calibrated to the measured RED for the Fluent simulation with a wall reflectivity of 40% at UVT = 88%, the simulated RED matches the measured RED for that run. Without wall reflection, the simulated RED for UVT = 88% is about 6% less. At UVT = 98.6%, the difference between the simulated REDs with and without reflection is about 23% (with a wall reflectivity of 40%). Also, the Fluent results with a wall reflectivity of 40% over predict the measured RED by ~18%, and the Fluent results without reflection under predict the measured RED by ~10%. The use of a lower wall reflectivity of 20% (as suggested by Keith Bircher from Calgon) is also shown in Figure 12. The reduced wall reflectivity of 20% does not change the simulated RED significantly for a UVT

= 88%. However, at UVT = 98.6%, the simulated RED is reduced by ~13% when the wall reflectivity is reduced from 40% to 20%, and the results match the data better (within 4%).

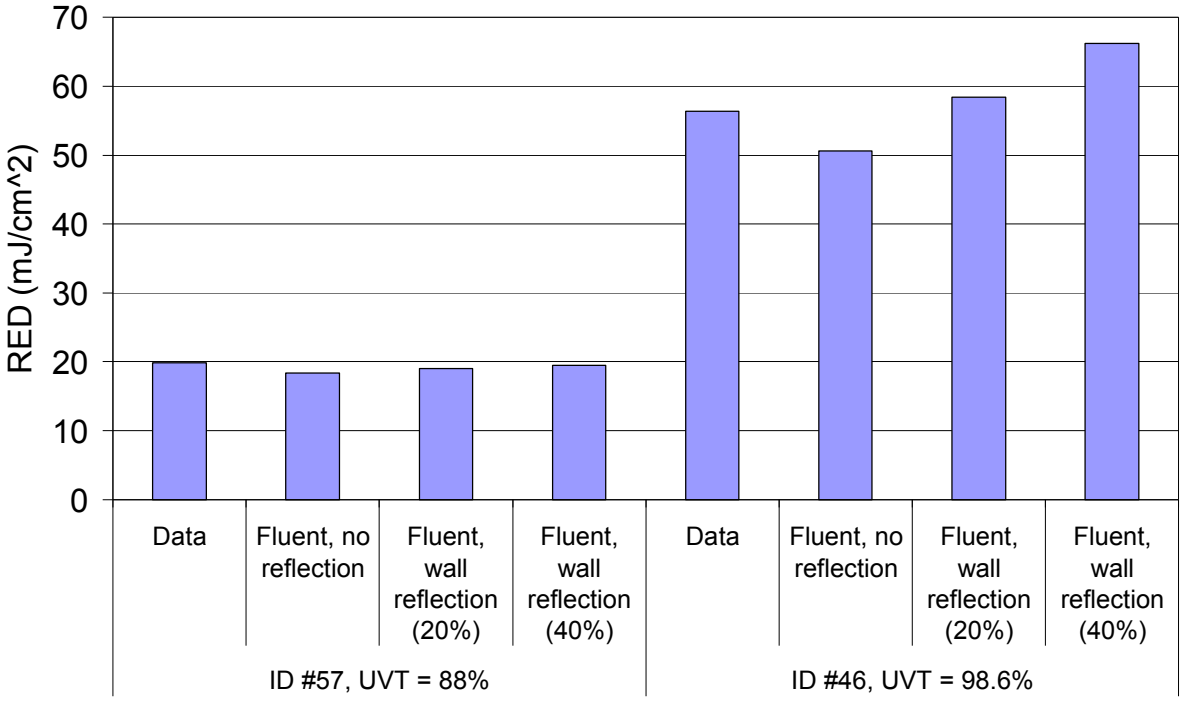

Figure 12. Comparison of measured vs. simulated RED using Fluent with and without reflection for UVT = 88% and UVT = 98.6% in the Calgon reactor.

SUMMARY AND CONCLUSIONS

The objective of this work was to determine important factors that impact the simulated reduction equivalent dose (RED) using CFD-based models of hydraulics, radiation, dose, and inactivation kinetics. A few sensitivity analyses highlighted in this paper included an investigation of particle tracking inputs and a study of the impact of wall reflection.

The particle tracking sensitivity study showed that for the IDI and Calgon reactor configurations simulated in this study, the use of at least 5,000 - 10,000 particles with any number of tries (when DRW was enabled) yielded minimal variability (less than 1-2 percent) in the simulated RED. However, a significant difference was observed between the simulated REDs when DRW was turned on vs. off, and this difference was found to be a function of flow rate. As the flow rate increases, the higher mean particle velocities dominate the normally distributed random velocity fluctuations used by the DRW model. As the flow rate decreases, the turbulent velocity fluctuations included in the DRW model become more dominant and significantly influence the predicted particle trajectories and the simulated RED.

The wall reflection sensitivity study revealed that the inclusion of wall reflection can increase the simulated UV irradiation by up to 100% within the reactor at high UVT (98.6%). At lower UVT (88%), the impact of wall reflections was much less (but still noticeable). Therefore, accounting for wall reflection may be important when trying to simulate UV dose in reactors with high UVTs and reflective surfaces.

ACKNOWLEDGMENTS

This work was funded by AwwaRF project #4107 "*Evaluation of Computational Fluid Dynamics (CFD) as a Cost-Effective Tool for Assessing UV System Performance*." Sandia is a multiprogram laboratory operated by Sandia Corporation, a Lockheed Martin Company for the United States Department of Energy's National Nuclear Security Administration under contract DE-AC04-94AL85000.

REFERENCES

Liu, D., Ducoste, J., Jin, S., and Linden, K., 2004. Evaluation of alternative fluence rate distribution models. Journal of Water Supply: Research and Technology—AQUA, 53.6, 391-408.

Luckiesh, M., 1929. Spectral reflectances of common materials in the ultraviolet region. *J. Optical Soc. America and Review of Scientific Intruments*, 19(1), 1-6.

Munoz, A., Craik, S. and Kresta, S., 2007. Computational fluid dynamics for predicting performance of ultraviolet disinfection - sensitivity to particle tracking inputs. *J. Environ. Eng. Sci.*, 6: 285-301.

Wicklein, E., Wright, H., and C. Ho, 2008. Computational fluid dynamics modeling of UV reactor validation tests, 2008 Water Quality Technology Conference, Cincinnati, OH, November 16-20, 2008.